SURVEY OF SWIMMING PATTERN CHANGES ASSOCIATED WITH THE SIZE OF CORTICAL INVERSIONS IN *PARAMECIUM TETRAURELIA*

An Undergraduate Research Scholars Thesis

by

ROBERT MICHAEL ANTON and SAM MICHAEL ANTON

Submitted to the Undergraduate Research Scholars program
Texas A&M University
in partial fulfillment of the requirements for the designation as an

UNDERGRADUATE RESEARCH SCHOLAR

Approved by
Research Advisor: Dr. Karl Aufderheide

May 2016

Major: Biology

TABLE OF CONTENTS

ABSTRACT

Survey of Swimming Pattern Changes Associated with the Size of Cortical Inversions in *Paramecium tetraurelia*

Robert Michael Anton and Sam Michael Anton
Department of Biology
Texas A&M University

Research Advisor: Dr. Karl Aufderheide
Department of Biology

The cell surface of *Paramecium tetraurelia* is covered in cilia organized into approximately 70 ciliary rows which extend from the anterior of the cell to the posterior. One or more of these ciliary rows can be surgically rotated 180^{o} in the local plane of the surface. These changes, known as cortical inversions, are heritable and produce rows of cilia which now have all of their anterior-posterior and left-right axes 180^{o}-rotated from that of normally positioned rows. The power stroke of the cilia in the inverted rows is also rotated, which produces an altered swimming track of the cell. We generated and characterized a series of cell lines with different sizes of cortical inversions, from 0 rows (wild-type control), up to approximately 20 rows (maximum observed size). The swimming track of each cell line was recorded and quantitatively measured. We developed a mathematical formula relating the number of ciliary rows that are inverted to the geometric characteristics of the helical path traced by the cell as it swims.

ACKNOWLEDGMENTS

We would like to thank Dr. Karl Aufderheide, it was through his patience and mentorship that we have been able to accomplish what I have.

NOMENCLATURE

KF: Kinetodesmal Fiber

BB: Basal Body

PS: Parasomal Sac

A/P: anterior/posterior

L/R: left/right

Invert: A paramecium exhibiting one or more inverted cortical rows

NJ: Narrow Juncture

WJ: Wide Juncture

CHAPTER I

INTRODUCTION

Paramecium is a genus consisting of unicellular and free-living protists that are widely distributed across the globe. Members of the Phylum Ciliophora, paramecia, are large in size, with different species ranging from 50 µm up to 300 µm in length. These protists are exceptionally complex cells as shown by their interior and surface organization.

In eukaryotic cells, cilia arise from basal bodies rooted in the cortex or cell surface. The “9x3” microtubular pattern shown by the basal bodies provide the template from which the “9+2” axonemal microtubules grow. The cortical organization of the cytoskeleton in ciliates positions the cilia in rows with anterior to posterior (A/P) polarity and left-right (L/R) asymmetry. Each cortical unit contains a stereotyped array of cytoskeletal and membranous components organized around one or two basal bodies, which are often ciliated (figure 1). *Paramecium tetraurelia* demonstrates this organization (Beisson 2008; Aufderheide, et al., 1980). The cilia beat in a whip-like fashion from anterior-right to posterior-left, in a coordinated fashion, propelling the cell forward. The direction of the ciliary power stroke means that the cell swims forwards in a left- handed helical track.

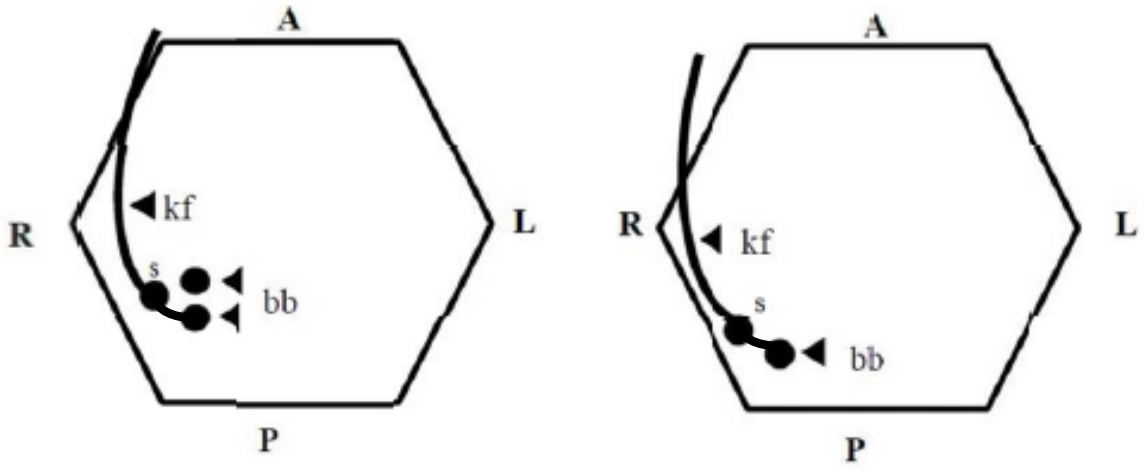

Fig. 1: A schematic representation of the *P. tetraurelia* cortical unit (Cross 2012). This illustrates the cytoskeletal components which include one or two ciliary basal bodies, a parasomal sac and a kinetodesmal fiber as seen when the cell is stained using the Fernández-Galiano method (Fernández-Galiano 1994). The basal bodies (bb) and parasomal sac (s) lie offset with regards to the center. Stemming from the posterior basal body, the kinetodesmal fiber (kf) arises at the basal body and extends anteriorly on the right side of the unit. These cortical units exhibit a well-defined polarity and asymmetry, in regards to both the A/P and the L/R directions. Note that left and right are defined from the viewpoint inside the cell, looking out, but, by convention, diagrams and micrograms are viewed from the outside of the cell.

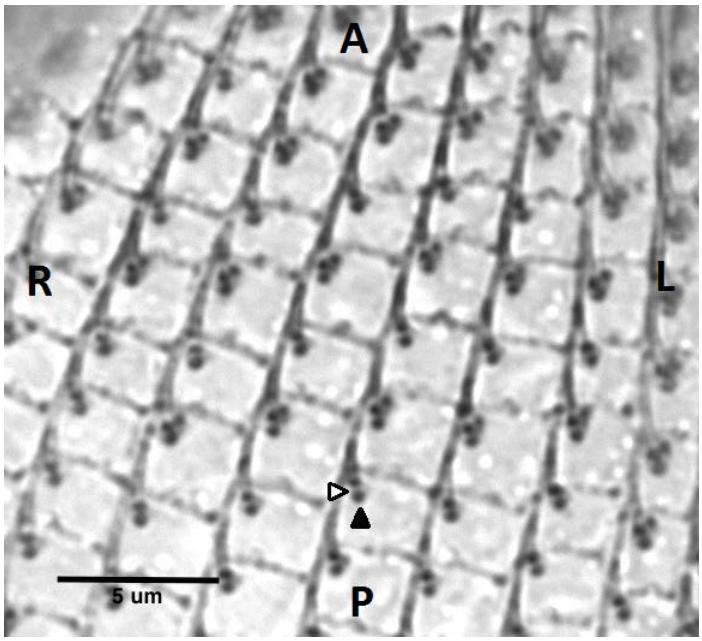

Fig. 2: Fernández-Galiano stain a portion of the cortex of a wild-type *Paramecium tetraurelia* (Fernández-Galiano 1994). The black arrow indicates a basal body from which the cilia extends. The white arrow points to the parasomal sac. The hair-like projections are kinetodesmal fibers which point towards the anterior end of the cell. The outlines of the alveolar sac represent the individual cortical units.

In *Paramecium* and closely related ciliates, it is possible to physically generate a cortical inversion, or a 180^{o} planar rotation of a region of the cortex, which thus reorients the A/P and L/R axes of one or more longitudinal rows of cilia (Aufderheide et al., 1999; Beisson and Sonneborn 1965). One consequence of these inverted ciliary rows is that the power strokes of inverted cilia are also rotated 180^{o}, meaning that affected cilia now beat from posterior-left to anterior-right. A consequence of one or more inverted ciliary rows present on a cell is a pronounced twisty swimming pattern, noticeably different from that of wild-type cells. The twisty swimming pattern has been observed to become more extreme as the number of cortical inversions per cell increases (Tamm 1975). A preliminary study by Bessellieu (2014)

demonstrated that the cells' swimming pattern could be related to the size of the cortical inversion on the cell's surface. Bessellieu's work suggested that the quantitative features of a cell's swimming path could potentially be quantitatively and mathematically related to the number of inverted ciliary rows.

Experimental hypothesis

This project was an effort to successfully culture and maintain cell lines with different sizes of inversions and to examine their swimming patterns, compared to that of the wild-type. To a casual observer, the difference in swimming patterns between the two cell types is apparent, as is a gradual progression from normal to moderate and finally extreme as the corticotype changes. We hypothesized, based on these observations, the observed changes in the swimming pattern in *P. tetraurelia* were quantifiable and could be described by a comprehensive mathematical formula which would relate the geometry of the cell's swimming path to the number of fully inverted ciliary rows that cell is carrying. By examining the time-exposure dark-field image of swimming cells (wild-type or cells with cortical inversions), it would be possible to predict the cell line's corticotype before staining. In order to formulate this mathematical equation, data was collected from a wide range of corticotypes.

Project objectives

i. We isolated and surveyed a series of cell lines with differing sizes of cortical inversions from 0 (wild-type/normal) up to the maximum observed size of 20 rows. We quantified the sizes of the inversions of each of the lines, and their locations on the cell, by corticotype characterization. The mathematical parameters of the different helical

swimming patterns in each of the cell lines with differing sizes of cortical inversions were measured, including the pitch of the helix, diameter of the helix, and cell velocity.

ii. We developed a mathematical algorithm which relates the number of inverted rows to the helical path that a cell traces as it swims.

CHAPTER II

METHODS

Culturing

Our wild-type cell lines were cultured by established techniques (Sonneborn, 1970; Beisson, et al., 2010). The cells were grown in a bacterized baked lettuce medium fortified with 5 mg/L stigmasterol and buffered with 5.25 mM sodium phosphate. The sterile medium was inoculated with a nonpathogenic strain of *Klebsiella pnumoniae* (ATCC #27889) and incubated at 37^{o}C several hours prior to use. Cells' culture records as well as transferring and handling procedures were accomplished by standard methods (Sonneborn, 1970; Beisson, et al., 2010).

Culturing inverted cell lines

The cell lines with cortical inversions had altered swimming capabilities (when contrasted with the wild-types) and collected food at a slower pace. As a result, the invert lines exhibited a longer cell cycle time and as a consequence, the cell lines containing inverts had to be selected and transferred to fresh medium (Sonneborn, 1970) more often in order to keep the cultures consistent and not overgrown with bacteria.

Staining and image capture

Cells were stained using a modified Fernández-Galiano silver carbonate technique (Fernández-Galiano 1994; Aufderheide, 2016, in press). We viewed the stained cells with an Olympus model microscope using bright-field optics. Images were taken using a Lumenera Scientific Infinity-2 camera. Image processing was done using the Image J software.

Corticotyping

In order to accurately determine the number and location of inverted cortical ciliary rows on our cell lines, corticotyping was employed. Corticotyping is a technique which involves counting the ciliary rows around the circumference of the paramecium starting from the first visible row on the left-hand side of the oral apparatus. By convention, left and right are defined from the perspective of being inside the cell and looking out. From the first visible ciliary row on the left side of the oral apparatus, the rows were counted in a counter-clockwise direction around the circumference of the cell until the right side of the oral apparatus was reached (completing the full 360^{o} rotation) (figure 3). The corticotype of each cell was described in a sequence of 3 numbers: a.b.c. The number of normal ciliary rows until the first inverted row was reached was recorded in the a value, the total number of inverted rows on the cell surface being denoted in the b value, and c was the value representing the total number of ciliary rows (both inverted and normal) on the surface of the cell not including those inside of the oral apparatus.

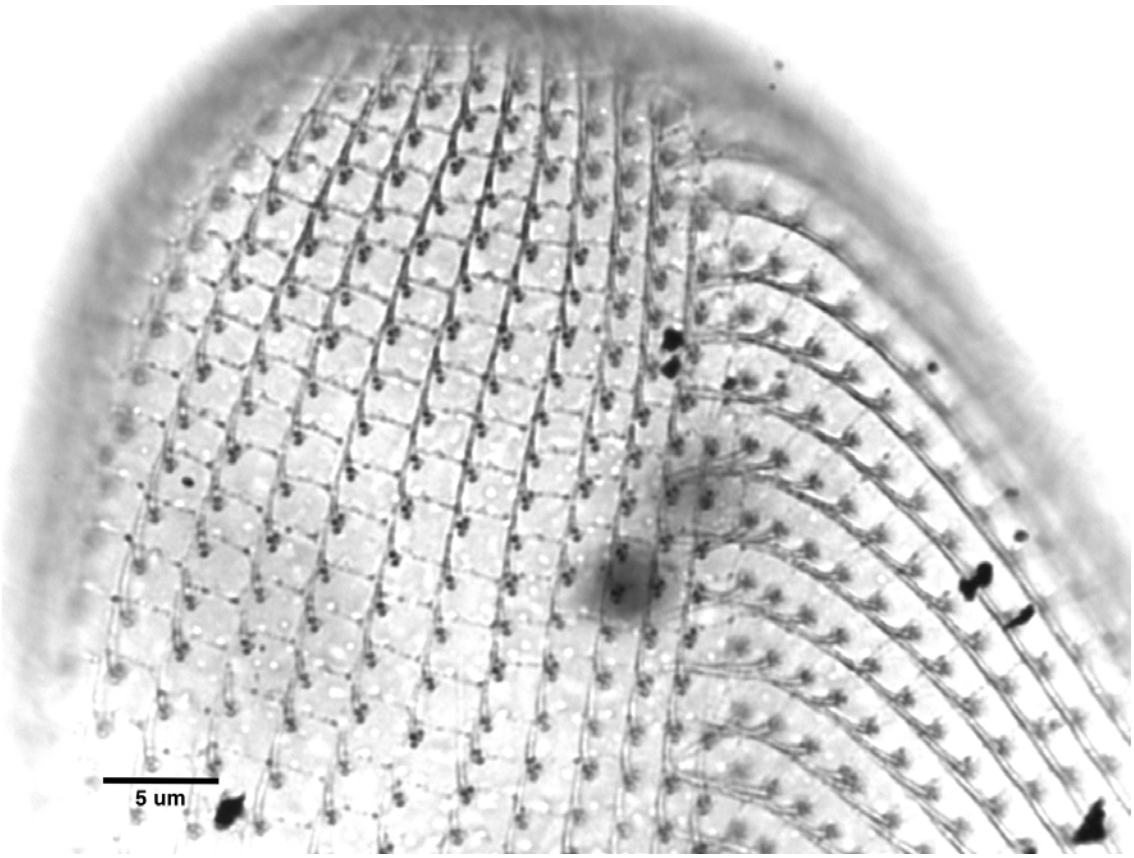

Fig. 3: Anterior suture of the *P. tetraurelia* cortex connects to the oral apparatus which is directly below, and central to the margin of this image.

Identifying the inversions

A cortical inversion could be identified while observing the stained cells with light-field microscopy. The right side of an inversion was marked by a wide juncture (WJ) (figure 4). This wide juncture is a direct result of the 180^{o} inversion of the entire cortical unit which displaces the orientation of the kinetodesmal fibers from the anterior-left to the posterior-right of the unit with regards to the cell's axes (figure 4). The left side of the inverted ciliary rows to normal rows is characterized by a narrow juncture (NJ) for the same reason as described regarding the WJ.

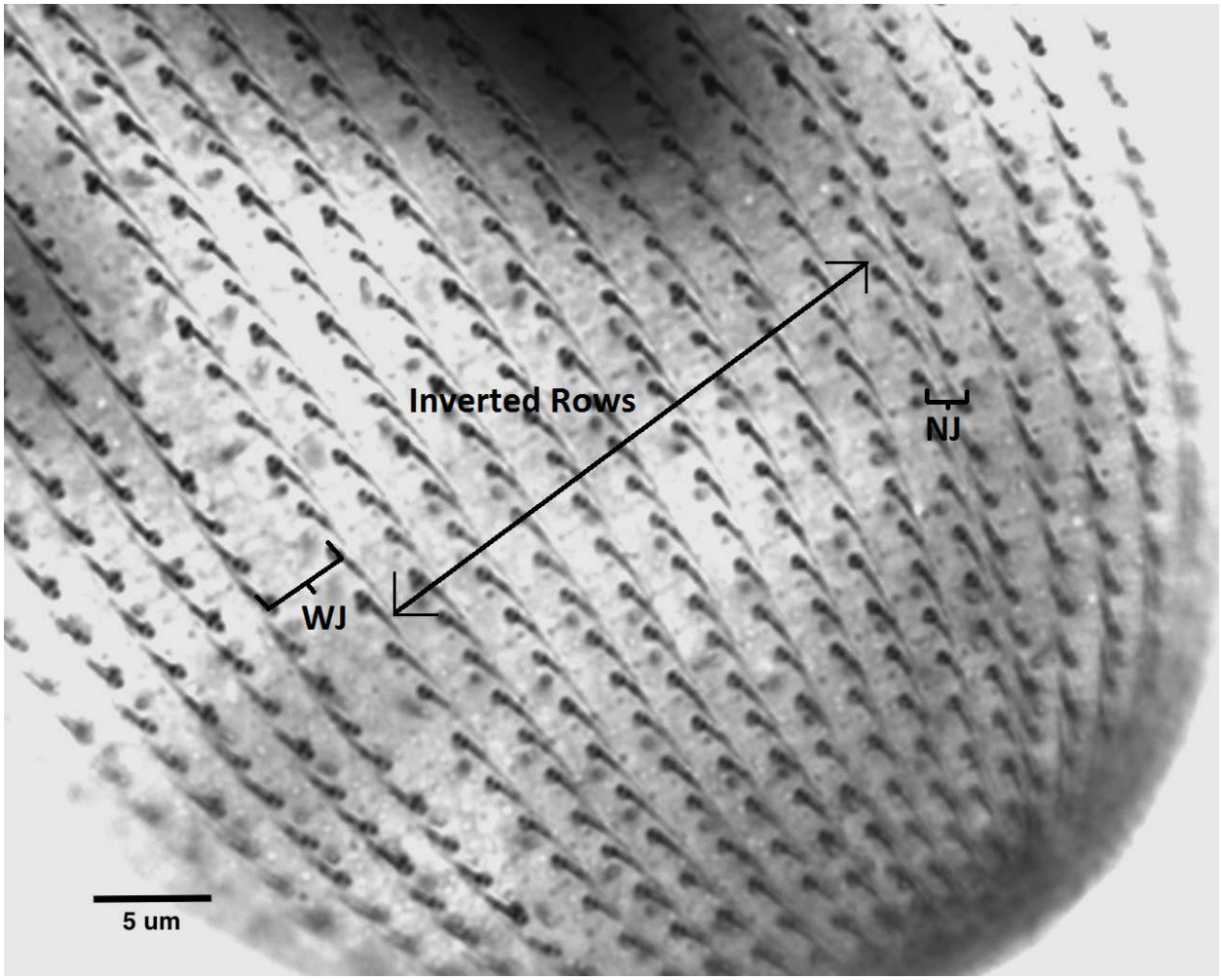

Fig 4: Image of the stained cortex of *P. tetraurelia*. Arrow one points to the wide juncture of cortex, which indicates the first inverted row on the particular cell. The left side of the image shows the left "shoulder" of the cell. Moving right from the wide juncture (WJ), the next eleven rows are inverted until one reaches the narrow juncture (NJ) where the normal rows resume.

Swimming track recording and analytical inference

Cells from each cell line that was isolated and corticotyped were transferred several times through Dryl's buffer at room temperature (Dryl 1959). The cells were then placed in a 6x6x1 mm "motility chamber" constructed on a glass slide. Dryl's was added to bring the depth in the

chamber to precisely 1 mm. The chamber was then observed using dark-field optics. Dark-field allowed the cells to be viewed as bright white units on a dark background (figure 5) and their swimming tracks followed suit. A Lumenera Scientific Infinity-2 camera was used to take two-second images. Twenty to twenty-five images were taken for each cell line and analyzed using Image J software for key variables: velocity, helical diameter of the track, vertical pitch and overall length.

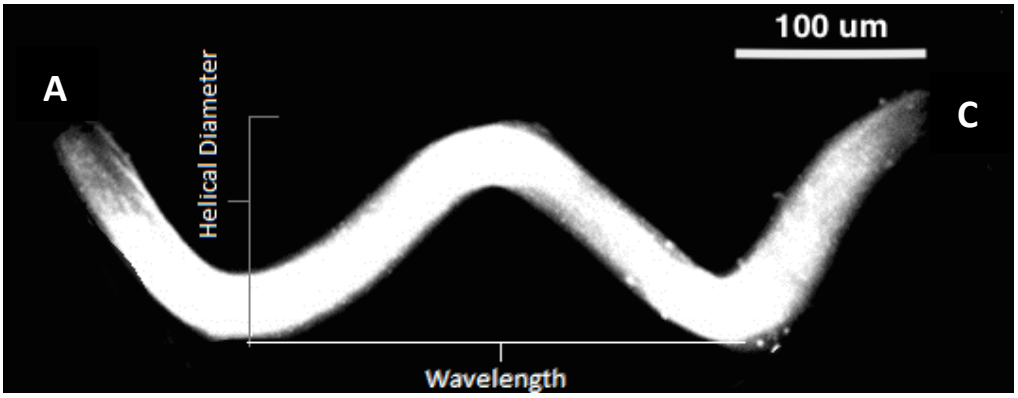

Fig. 5: A two-second swimming track image of *P. tetraurelia* with approximately 6.5 inverted rows on its surface. Dozens of images similar to these were collected and examined for the parameters necessary to accurately derive a formula.

Wavelength was calculated by measuring the distance between two adjacent peaks. Helical diameter was calculated by measuring the distance between one extreme of the wave form to the other. The overall length was measured simply by the distance between one end of the track (labeled A) to the other (labeled C) during the 2 sec exposure. The velocity was determined by dividing the overall distance by the length of time of the exposure, 2 seconds. All measurements were recorded in micrometers, and the velocities were in units of micrometers/second.

Mathematical analysis

Standard statistical methods were used to analyze data (Sokal and Rholf 1969). We utilized all of the data points we had collected from both our corticotyping and corresponding swim track analysis and compared their relationships in a graphical way using SAS Enterprise Model software. The software examined all possible modeling methods and deduced that using simple linear regression to relate the average number of inverted rows (collected from the corticotype data) to the three parameters of interest from the swimming track analysis would produce the most accurate predictive formula. With this knowledge, three linear regressions were produced (figures 8-10) and their respective formulas combined around the basis of a common y-axis variable (inverted rows). Testing was done on the formula to confirm its accuracy.

CHAPTER III

RESULTS AND DISCUSSION

Examining corticotypes

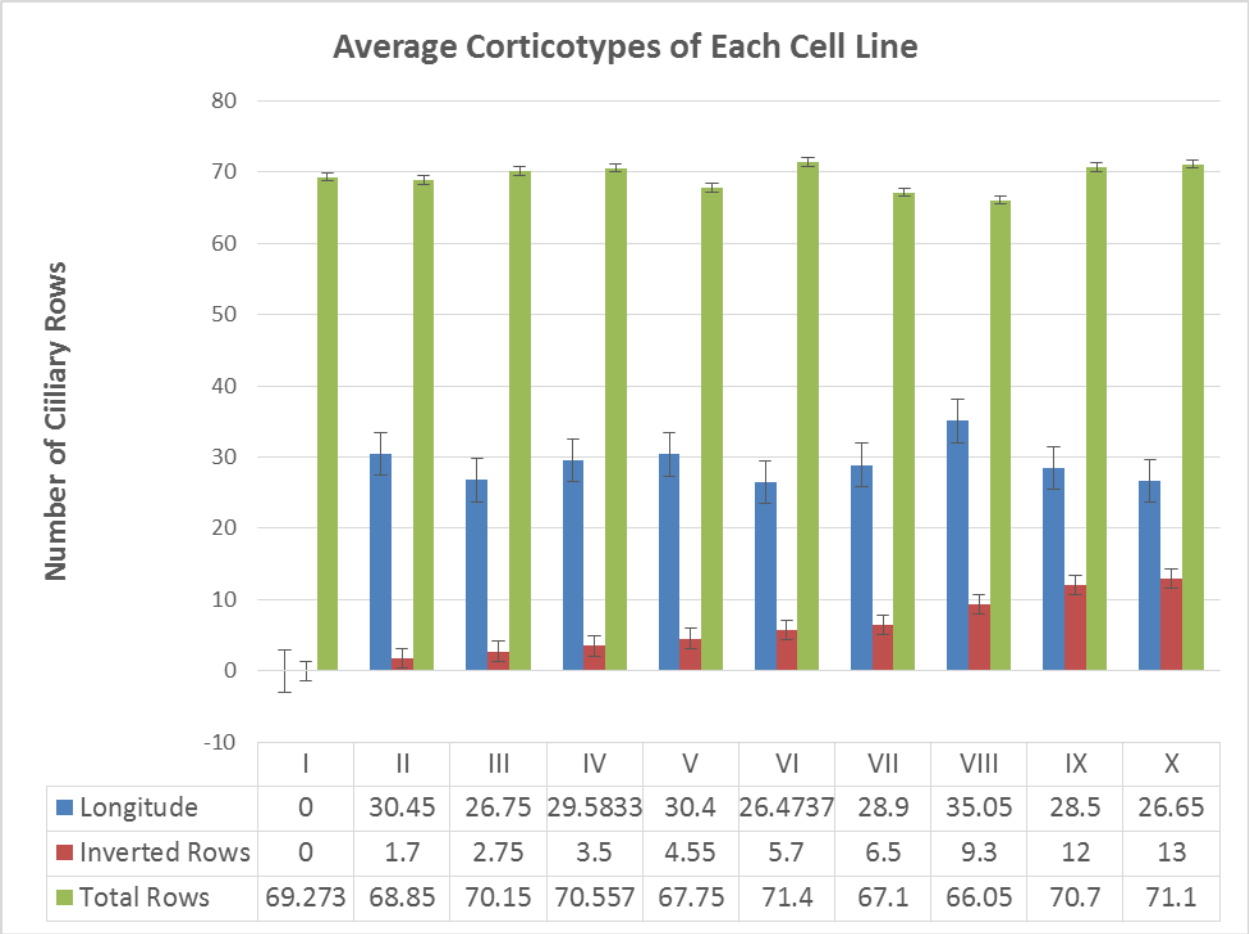

	I	II	III	IV	V	VI	VII	VIII	IX	X
Longitude	0	30.45	26.75	29.5833	30.4	26.4737	28.9	35.05	28.5	26.65
Inverted Rows	0	1.7	2.75	3.5	4.55	5.7	6.5	9.3	12	13
Total Rows	69.273	68.85	70.15	70.557	67.75	71.4	67.1	66.05	70.7	71.1

Fig. 6 A graphical representation of the average corticotype data collected across ten different cell lines ranging from wild type, cell line I, with zero inversions, up to max inverts, cell line X, with an average of 13 cortical rows inverted (standard error bars included). The green bar represents the total number of rows, the blue bar is representative of the longitude (the number of rows counted up to the first inverted row) and finally the red bar represents the average numer of inverted rows of each of the representative lines.

Figure 6 illustrates the wide extent of possible corticotypes in *P. tetraurelia*. It also identifies the average number of inverted rows in each respective cell line as well as the location of the inversion with respect to the cortical geography (longitude). We see that regardless of the number of inverted rows present on the cortical surface, the longitudinal location of the inversions are consistent, meaning that each of the of inversions are localized in the same position on the cell (which is the “back left shoulder”). This consistency of longitude removes it as a variable in determining the effect of the inversions on swimming pattern. The consistency in number of total ciliary rows across all cell lines also removes it as a possible variable responsible for resulting in different cell swimming tracks.

Swimming track inference

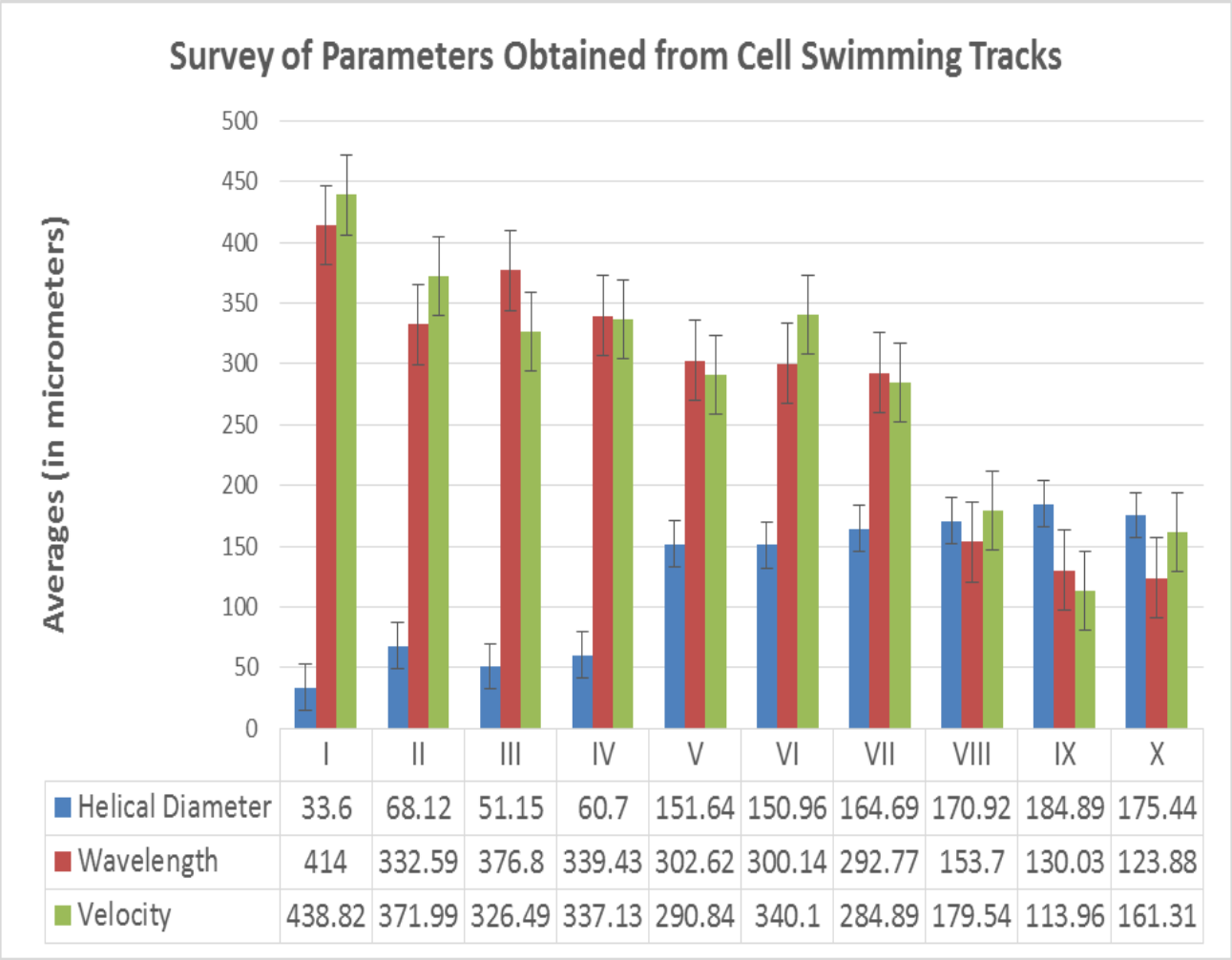

	I	II	III	IV	V	VI	VII	VIII	IX	X
Helical Diameter	33.6	68.12	51.15	60.7	151.64	150.96	164.69	170.92	184.89	175.44
Wavelength	414	332.59	376.8	339.43	302.62	300.14	292.77	153.7	130.03	123.88
Velocity	438.82	371.99	326.49	337.13	290.84	340.1	284.89	179.54	113.96	161.31

Fig. 7: A bar graph depicting the trends in the changes of our parameters as they relate to the changes in the mean number of inverted ciliary rows which are given by the specific cell line I-X seen in figure 6. Standard error bars are displayed. The parameters are described as follows, the green bars show velocity, the red shows wavelength and the blue shows the helical diameter. The first parameters, velocity is given in units of μm/s; whereas, the other two parameters wavelength and helical diameter are described in units of μm

Figure 7 show a summary of the data collected from the swimming track images taken for each cell line. The parameters of interest: helical diameter, wavelength, and velocity were all recorded and are denoted in the table below the figure. Using least squares linear regression, there is an inverse relationship between the two parameters velocity and wavelength and the number of cortical inversions displayed by the cell (Figures 8 and 9). Contrarily, there is a positive linear relationship which links the mean number of cortical inversions to the mean helical diameter of the swimming tracks (Figure 10). These three relationships were modeled and compared using SAS Enterprise Miner software from which we constructed a predictive formula (Figure 11).

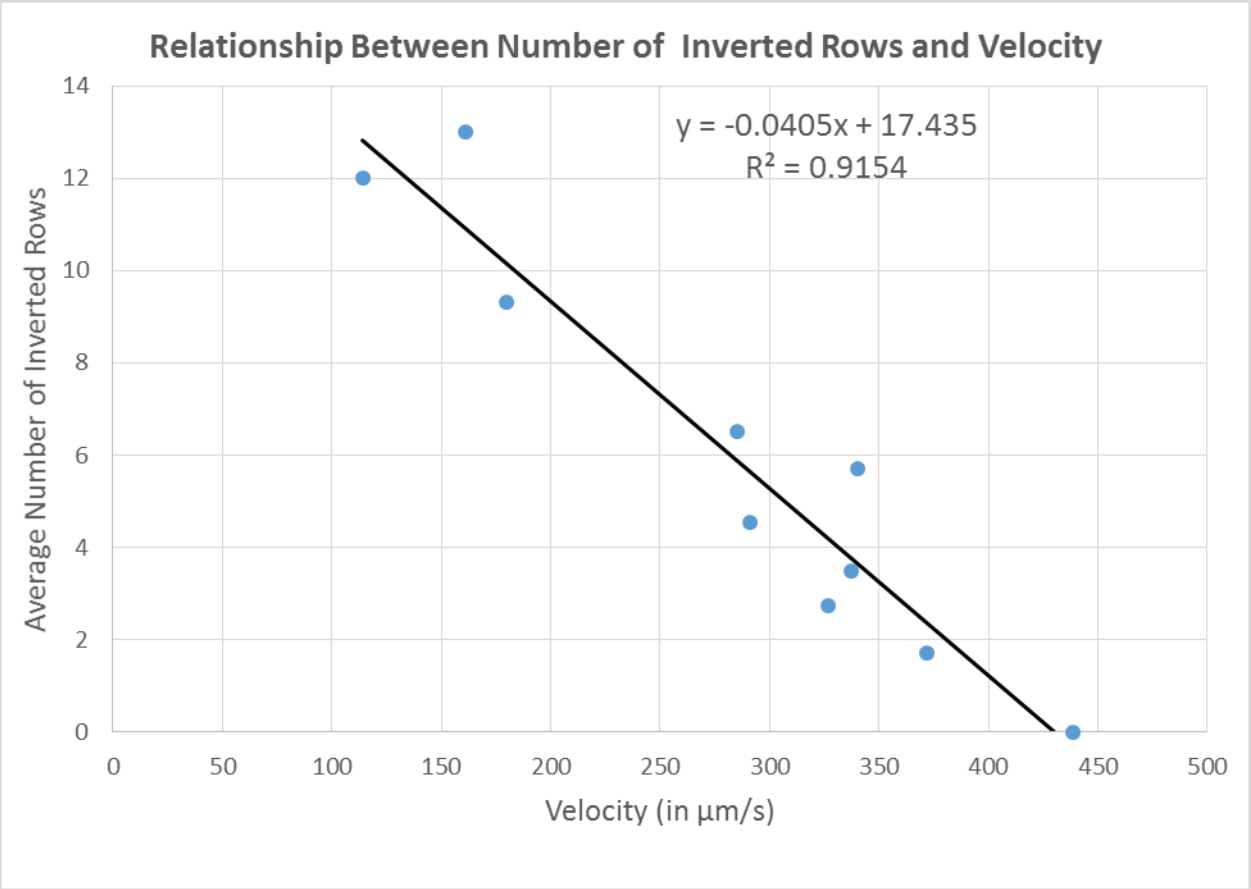

Fig. 8: Graphical interpretation of the relationship between the average number of inverted ciliary rows and the velocity of the cell as it swims. This is a negative linear relationship.

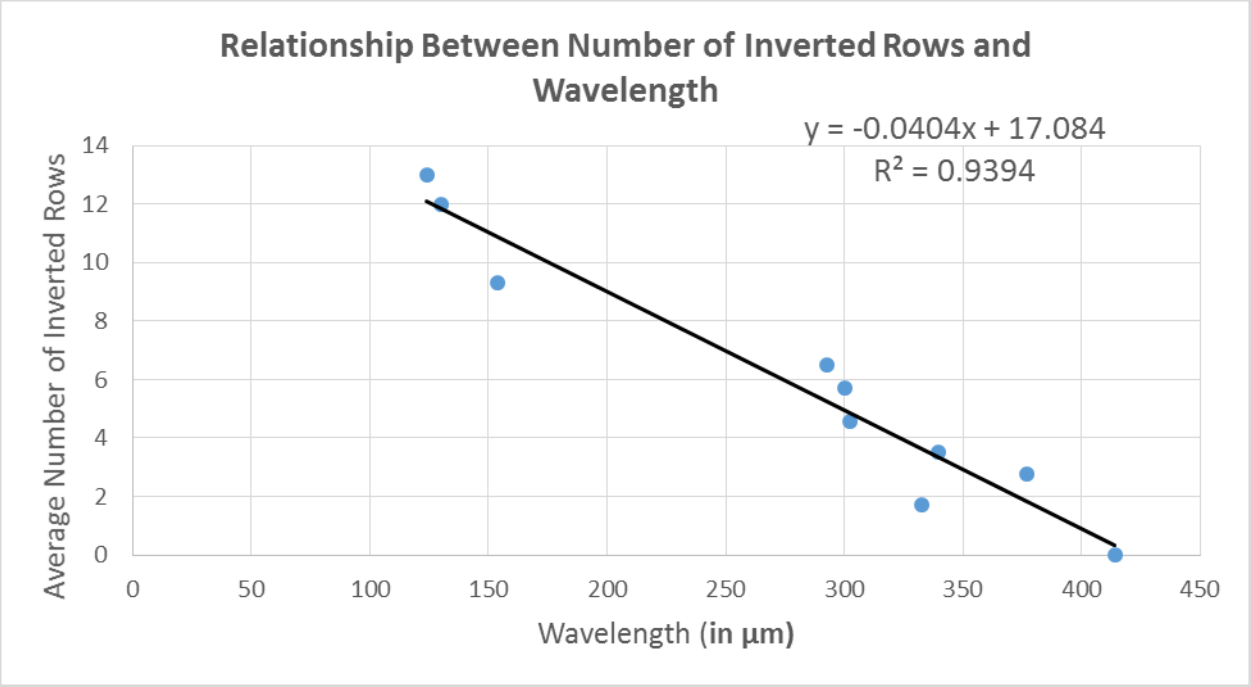

Fig. 9: Graphical interpretation of the relationship between the average number of inverted ciliary rows and the wavelength of the cell as it swims. This is a negative linear relationship.

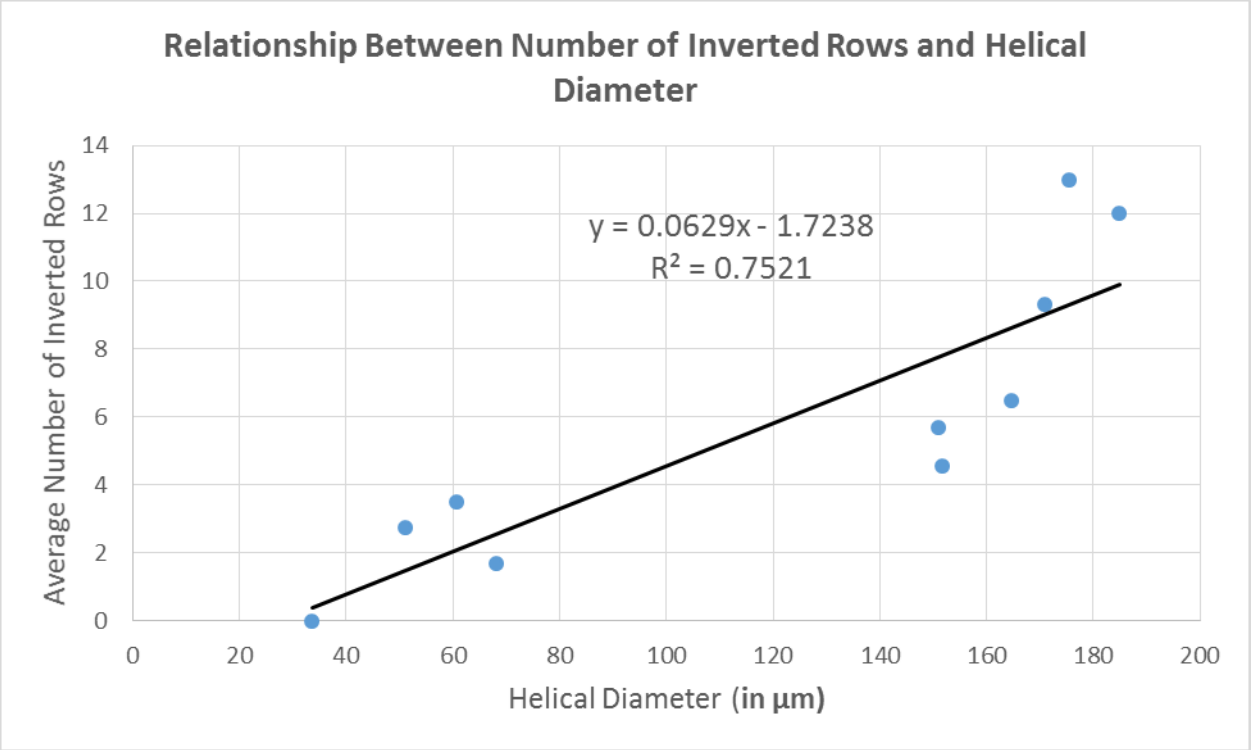

Fig. 10: Graphical interpretation of the relationship between the average number of inverted ciliary rows and the helical diameter of the cell as it swims. This is a positive linear relationship

Cell Line	Longitude	Inverted Rows	Total Rows
I	0	0	69.273
II	30.45	1.7	68.85
III	26.75	2.75	70.15
IV	29.583333	3.5	70.557
V	30.4	4.55	67.75
VI	26.47368	5.7	71.4
VII	28.9	6.5	67.1
VIII	35.05	9.3	66.05
IX	28.5	12	70.7
X	26.65	13	71.1

Fig. 11: Average corticotyping data for cell lines I through X.

Cell Line	Helical Diameter	Wavelength	Velocity
I	33.6	414	438.82
II	68.12	332.59	371.99
III	51.15	376.8	326.49
IV	60.7	339.43	337.13
V	151.64	302.62	290.84
VI	150.96	300.14	340.1
VII	164.69	292.77	284.89
VIII	170.92	153.7	179.54
IX	184.89	130.03	113.96
X	175.44	123.88	161.31

Fig. 12: Average swimming track data for cell lines I through X.

Predictive formula

$$IR = \frac{(-0.0405)v}{3} + \frac{(-0.0404)\lambda}{3} + \frac{(-0.0692)\delta}{3} + 10.9317$$

Fig. 13: IR: number of inverted rows**, v**: velocity of cell**, λ**: wavelength**, δ**: helical diameter

The predictive formula shown above is the result of standard statistical methods typically employed for mass quantities of data. Each of the three parameters, velocity, wavelength and helical diameter are represented in this model which increases the overall accuracy of the formula which has been tested across hundreds of potential data sets.

CHAPTER IV

CONCLUSION

Implications of the formula

We were able to successfully create a formula which could act as a predictive model in ciliary swimming patterns for *P. tetraurelia.* The formula can be used as a basis for hypothesis generation and testing of other mathematical formulas which could possibly predict a whole array of swimming mechanics in a variety of other organisms or mechanical systems which exhibit helical patterns of movement. Although there has been other mathematical analysis of the mechanism of ciliary motion, there has been little specific work on the production of helical movement through media, so our findings are significant to an understanding of the mechanisms of protist swimming.

Applications of the formula

The formula that we have derived from our data serves a dual purpose. Not only could one utilize it in order to estimate the number of inverted ciliary rows of a cell whose corticotype is unknown by examining its swimming track, but it could potentially serve as a basis for further mathematical analysis of swimming patterns in other species of ciliates.

REFERENCES

Aufderheide, K. J., T. C. Rotolo, and G. W. Grimes. (1999): Analysis of inverted ciliary rows in *Paramecium.* Combined light and electron microscopic observations. Europ. J. Protistol. **35**:81–91.

Beisson, J. (2008): Preformed cell structure and heredity. Prion **2**:1–84

Beisson, J. and Sonneborn, T. M. (1965) Cytoplasmic inheritance of the organization of the cell cortex in *Paramecium aurelia.* Proc. Natl. Acad. Sci. **53**:275–282.

Beisson, J., Bétermier, M., Bré, M.-H., Cohen, J., Duharcourt, S., Duret, L., Kung, C., Malinsky, S., Meyer, E., Preer, J. R., Jr., and Sperling, L. (2010) Maintaining clonal *Paramecium tetraurelia* cell lines of controlled age through daily reisolation. Cold Spring Harb. Protoc. DOI: 10.1101/pdb.prot5361.

Bessellieu, J. B. (2014): Structural inheritance and swimming pattern in *Paramecium tetraurelia* cells with cortical inversions. Texas A&M Honors Undergraduate Research Thesis.

Cross, R. K. (2012): Analysis of the heritability of cortical inversions through sexual exchange in *Paramecium tetraurelia.* Texas A&M Honors Undergraduate Research Thesis.

Dryl SJ. (1959): Antigenic transformation in *Paramecium aurelia* after treatment during autogamy and conjugation. J Protozool **6**: S25

Fernández-Galiano D. (1994): The ammoniacal silver carbonate method as a general procedure in the study of protozoa from sewage (and other) waters. Wat. Res. **28**:495–496.

Sokal, R. R., and Rholf J. F. (1969): *Biometry: The Principles and Practice of Statistics in Biological Research*. W. H. Freeman and Company New York, 915 pp.

Sonneborn, T. M. (1970): Methods in *Paramecium* research. Methods Cell Physiol. **4**:241–339.

Tamm, S.L., T. M. Sonneborn, and R. V. Dippell. (1975): The role of cortical organization in the control of ciliary beat in *Paramecium.* J. Cell Biol. **64**:98–112